Aromatic Residues at the Extracellular Ends of Transmembrane Domains 5 and 6 Promote Ligand Activation of the G Protein-Coupled α-Factor Receptor†

Jennifer C. Lin,‡,§ William Parrish,§,|| Markus Eilers,⊥ Steven O. Smith,⊥ and James B. Konopka*,§

Graduate Program in Molecular and Cellular Biology, State University of New York, Stony Brook, New York 11794, Department of Molecular Genetics and Microbiology, State University of New York, Stony Brook, New York 11794-5222, and Department of Biochemistry and Cell Biology, Center for Structural Biology, State University of New York, Stony Brook, New York 11794

Received August 30, 2002; Revised Manuscript Received October 25, 2002

ABSTRACT: The α-factor receptor (*STE2*) stimulates a G protein signaling pathway that promotes mating of the yeast *Saccharomyces cerevisiae*. Previous random mutagenesis studies implicated residues in the regions near the extracellular ends of the transmembrane domains in ligand activation. In this study, systematic Cys scanning mutagenesis across the ends of transmembrane domains 5 and 6 identified two residues, Phe^{204} and Tyr^{266}, that were important for receptor signaling. These residues play a specific role in responding to α-factor since the F204C and Y266C substituted receptors responded to an alternative agonist (novobiocin). To better define the structure of this region, the Cys-substituted mutant receptors were assayed for reactivity with a thiol-specific probe that does not react with membrane-imbedded residues. A drop in reactivity coincided with residues likely to be buried in the membrane. Interestingly, both Phe^{204} and Tyr^{266} are located very near the interface region. However, these assays predict that Phe^{204} is accessible at the surface of the receptor, consistent with the strong defect in binding α-factor caused by mutating this residue. In contrast, Tyr^{266} was not accessible. This correlates with the ability of Y266C mutant receptors to bind α-factor and suggests that this residue is involved in the subsequent triggering of receptor activation. These results highlight the role of aromatic residues near the ends of the transmembrane segments in the α-factor receptor, and suggest that similar aromatic residues may play an important role in other G protein-coupled receptors.

The α-factor receptor (Ste2p) stimulates mating in *Saccharomyces cerevisiae* (*1*, *2*). Like other members of the G protein-coupled receptor (GPCR)[1] superfamily, the α-factor receptor is comprised of seven transmembrane domains (TMDs) connected by extracellular and intracellular loops (*3*). The binding of the tridecapeptide α-factor pheromone (WHWLQLKPGQPMY) to its receptor activates a heterotrimeric G protein that leads to the stimulation of a MAP kinase pathway (*4*−*6*). Although the components of this signaling cascade are conserved from yeast to humans (*1*, *2*), the sequence of the α-factor receptor is not significantly homologous with other members of the GPCR family. Despite this, mutational analysis indicates that there is underlying structural and functional similarity between the α-factor receptor and other GPCRs (*7*, *8*). Furthermore, the α-factor receptor can activate mammalian $G\alpha_{olf}$ subunits (*9*), and certain mammalian GPCRs can activate the pheromone-responsive G protein pathway in yeast (*10*, *11*).

Ligand binding strategies vary widely in the GPCR family, consistent with these receptors responding to a variety of ligands ranging from small molecules to large glycoproteins (*12*). The α-factor receptor is similar to other GPCRs in that the core region composed of the seven TMDs is essential for ligand binding and G protein activation (*13*, *14*). The analysis of interspecies chimeras of the α-factor receptor first implicated the extracellular domains in α-factor binding specificity (*15*). More recently, analysis of a collection of dominant-negative mutants of *STE2* suggested that the extracellular ends of the TMDs play a special role in receptor signaling (*16*−*18*). These mutant receptors are strongly defective in responding to α-factor and appear to dominantly interfere with the ability of wild-type receptors to signal by sequestering the G proteins (*19*). The residues affected by the dominant-negative mutations are all predicted to be near the extracellular ends of the TMDs. This profile was unique to the dominant-negative mutants as other types of α-factor receptor mutants, such as constitutive mutants, are not all clustered at the ends of the TMDs (*7*, *20*).

† This work was supported by National Institutes of Health Grant GM55107 awarded to J.B.K.

* To whom correspondence should be addressed. E-mail: james.konopka@sunysb.edu. Phone: (631) 632-8715. Fax: (631) 632-9797.

‡ Graduate Program in Molecular and Cellular Biology.

§ Department of Molecular Genetics and Microbiology.

|| Current address: Division of Cellular and Molecular Medicine, Howard Hughes Medical Institute, University of California at San Diego School of Medicine, La Jolla, CA 92093.

⊥ Department of Biochemistry and Cell Biology, Center for Structural Biology.

[1] Abbreviations: GPCR, G protein-coupled receptor; TMD, transmembrane domain; MTSEA-biotin, 2-[(biotinoyl)amino]ethyl methanethiosulfonate; novobiocin, *N*-(7-{[3-*O*-(aminocarbonyl)-6-deoxy-5-*C*-methyl-4-*O*-methyl-β-L-lyxo-hexopyranosyl]oxy}-4-hydroxy-8-methyl-2-oxo-2*H*-1-benzopyran-3-yl)-4-hydroxy-3-(3-methyl-2-butenyl)-benzamide.

10.1021/bi026766o CCC: $25.00
Published on Web 12/20/2002

The observation that the dominant-negative *STE2* mutants affected 13 different residues near the predicted extracellular ends of the TMDs strongly suggested that they could be identifying a key functional domain that is important for ligand binding and receptor activation. Interestingly, the extracellular regions, including the ends of the TMDs, have also been implicated in the binding of peptide ligands by other GPCRs (*12*). However, further interpretation is limited because the precise ends of the TMDs are not known. Therefore, in this study, we set out to better define the domain composed of the extracellular ends of the TMDs. In particular, the ends of TMD5 and TMD6 were investigated since they are linked by the third intracellular loop, which plays a key role in G protein activation (*21*, *22*). Cys scanning mutagenesis was first used to identify residues that are important for receptor function. A variation of the substituted cysteine accessibility method (*23*) was then used to test the ability of the Cys residues to react with a membrane-impermeable probe. The results indicate that aromatic residues at the extracellular interface play a key role in ligand binding and receptor signaling. These results also have implications for the analysis of other GPCRs, and these methods may be generally applicable to the analysis of the TMD interface region in other membrane proteins.

MATERIALS AND METHODS

Strains and Media. Yeast strains yLG123 (*MAT*a *ade2-1^o his4-580^a lys2^o trp1^a tyr1^o leu2 ura3 SUP4-3^{ts} bar1-1 mfa2::FUS1-lacZ ste2::LEU2*), 7416-6-3 (*MAT*a *ade2-1^o his4-580^a lys2 tyr1 CAN CYH cry1 SUP4-3^{ts} leu2 ura3 ste2::LEU2 sst2-1*), and JKY25 (*MAT*a *ade2-1 his4-580^a lys2^o trp1^a tyr1^o leu2 ura3 SUP4-3^{ts} bar1-1 mfa2*::*FUS1-lacZ*) were used for the analysis of receptor mutants. Strain lys1α (*MAT*α *lys1*) was used for mating tests. Cells were grown in media as described previously (*24*). Yeast transformations were performed using the lithium acetate method (*25*). Plasmid-containing cells were grown in synthetic medium containing adenine and amino acid additives, but lacking uracil to select for plasmid maintenance.

Cysteine Scanning Mutagenesis. Plasmid pPD225-T7 (YEp-URA3-STE2-T7-3XHA) was used as a starting vector to create a set of Cys substitution mutants (*8*). This plasmid carries a modified *STE2* in which the two endogenous Cys residues at positions 59 and 252 were substituted with other amino acids, and it is also C-terminally tagged with a triple-HA epitope. This version of the receptor lacking Cys residues was used as the wild type for this study. Site-directed mutagenesis was carried out using a QUICK CHANGE kit (Stratagene). Mutagenic oligonucleotides were designed according to the manufacturer's instructions and were complementary to the *STE2* sequence except for the substitutions required to change codons 199−208 in TMD5 and 267−275 in TMD6 to encode Cys. The *STE2-A265C*, *-Y266C*, *-I209C*, *-L210C*, *-L211C*, *-A212C*, *-S213C*, and *-S214C* mutants were previously created on pPD225 (*8*). All mutations were confirmed by DNA sequence analysis using the Big Dye cycle sequencing kit (Applied Biosystems Inc.).

Reaction with MTSEA-Biotin. To assay reactivity with MTSEA-biotin {2-[(biotinoyl)amino]ethyl methanethiosulfonate} (Biotium), logarithmic-phase cells (10^8) were harvested by centrifugation and lysed by agitation with glass beads in 250 μL of cold PBS [10 mM Na_2HPO_4, 1.5 mM KH_2PO_4, 3 mM KCl, and 150 mM NaCl (pH 7.4)]. The lysate was cleared by centrifugation at 100*g* for 1 min, and then membranes were harvested by centrifugation at 15000*g* for 30 min. The membrane pellet was resuspended in 200 μL of PBS and then incubated with MTSEA-biotin (final concentration of 0.1 mM) at room temperature for 2 min. The MTSEA-biotin was freshly prepared in dimethyl sulfoxide at a final concentration of 20 mM. Reactions were quenched by addition of freshly prepared Cys to a final concentration of 10 mM and mixtures incubated for 5 min. Membrane proteins were then extracted in RIPA buffer [0.1% SDS, 1% Triton 100, 0.5% deoxycholic acid, 1× PBS (pH 7.4), and 1 mM EDTA]. Biotinylated proteins were harvested using UltraLink Immobilized Streptavidin Plus beads (Pierce) and eluted using gel sample buffer (8 M urea, 50 mM Tris, 2% SDS, and 10% 2-mercaptoethanol). Assays carried out in the presence of α-factor were performed in a similar manner except that the membrane pellet was incubated with 6×10^{-5} M α-factor (Bachem).

α-Factor Receptor Analysis. Western blots were carried out as described previously (*13*). Gel samples separated by electrophoresis on a 10% SDS−polyacrylamide gel were electrophoretically transferred to a Hybond-P membrane (Amersham Pharmacia Biotech). To detect the HA-tagged receptor proteins, the blots were probed with anti-HA antibody 12CA5 (Roche Molecular Biochemicals). Immunoreactive proteins were detected using alkaline phosphatase-conjugated goat anti-mouse IgG (Zymed) and an AttoPhos AP Fluorescent Substrate System (Promega). Quantitative analysis was carried out using ImageQuant computer software. As a control, wild-type and *STE2-T199C* cells were analyzed in parallel with the other mutants. Results for each mutant were calculated as the degree of biotinylation relative to T199C receptors. To detect biotinylation of proteins in the total membrane extract, the blots were probed with HRP-conjugated streptavidin (Amersham Pharmacia Biotech). The results were detected by chemiluminescence using 5-amino-2,3-dihydro-1,4-phthalazinedione as a substrate (Sigma).

Ligand-Induced Responses. Mating assays were carried out by mixing yeast strain yLG123 (*MAT***a** *ste2*Δ) containing the indicated wild-type or Cys-substituted mutant version of *STE2* on a plasmid with *MAT*α strain lys1α cells and then selecting for the growth of diploid cells. Halo assays for cell division arrest were performed by spreading on solid medium plates 6×10^5 yLG123 yeast cells carrying either a wild-type or the indicated mutant receptor gene on a plasmid, and then placing sterile filter disks containing either α-factor or novobiocin (Sigma) on the lawn of cells. Cells were grown at 30 °C for 48 h, and then the diameters of the zones of ligand-induced cell division arrest were measured.

Molecular Modeling. A molecular model of the α-factor receptor was generated by homology with the crystal structure of rhodopsin (*26*). The α-factor receptor is a member of the class D GPCRs. Only the class E receptors, which includes the *Drosophila* frizzled and smoothened receptors, are more divergent from rhodopsin. As a result, the α-factor receptor does not have many of the features characteristic of the consensus class A GPCR, including the ERY or DRY sequence on TMD3, the NPXXY sequence on TMD7, or the disulfide bridge between the extracellular end of TMD3 and the second extracellular loop. Neverthe-

less, the α-factor receptor has seven TMDs, and a comparison of the conserved and functionally important residues is sufficient for aligning the sequences in a meaningful way for developing a three-dimensional model.

The rotational orientations of TMDs were defined by potential pairwise interactions involving "functional domains" within the transmembrane helices. The most revealing amino acids are Glu, Gln, and Arg, which have long, highly polar side chains. These amino acids must be oriented toward the protein interior where they can participate in interhelical hydrogen bonding interactions (*27*, *28*). The translational positions of the helices were also constrained by specific pairwise helix−helix contacts as well as by the accessibility data that are presented, the location of positively charged Arg and Lys residues that are known to define the membrane boundary and Trp and Tyr which often partition in the region of the membrane headgroups (*29*, *30*). Computer programs used to predict the boundaries of the TMDs of the α-factor receptor were obtained from the ExPASy molecular biology server (http://ca.expasy.org/).

The key constraints defining the rotational and translation positions of the helices are as follows. For TMD1, Arg^{58} is oriented in toward the protein interior and is in a position to interact with Glu^{143} on TMD3. This orientation also leads to an inward orientation of Ser^{47} and Thr^{48}. For TMD2, Asn^{84} and His^{94} are oriented toward the protein interior. Asn^{84} is in a position to interact with Gln^{149} on TMD3 (*7*), while His^{94} may interact with Glu^{143}. In related α-factor receptors where Arg^{58} is replaced with His, His^{94} is replaced with Arg. Gln^{149} appears to be functionally equivalent to Glu^{134} at the cytoplasmic end of TMD3 in rhodopsin. Both Gln^{149} in Ste2p and Glu^{134} in rhodopsin are residues where mutation leads to constitutive activation. The rotational orientation of TMD3 is further constrained by Glu^{143}. Glu^{143} is conserved across the members of the α-factor receptor family and may interact directly or indirectly with Arg^{58} on TMD1 and/or His^{94} on TMD2. Glu^{143} in Ste2p is in a position similar to that of Glu^{122} in rhodopsin in the middle of TMD3. Glu^{143}, Arg^{58}, and His^{94} have roughly the same translation position in the model and are in proximity.

The rotational orientation of TMD4 is defined by Tyr^{181} which when replaced with Asn results in a loss of function (*18*). This orientation also places Ser^{170}, Gly^{174}, and Thr^{177} in the TMD3−TMD4 interface. Recently, we have found that small and polar residues have high propensities for occurring in helix interfaces (*31*).

The rotational orientation of TMD5 is defined by several positions that are thought to be in the TMD5−TMD6 interface. Substitution of Asn^{216} and Leu^{226} with Asp and Trp, respectively, results in constitutive activity (unpublished data and ref *32*). Val^{223} on TMD5 and Leu^{247} on TMD6 when changed to Cys are able to form a disulfide link (*8*). Finally, the position corresponding to Ala^{265} is an Asp in the homologous *mam2* receptor from *Schizosaccharomyces pombe* (*33*) and is a His in the a homologous receptor detected in the *Candida albicans* genome database (http://sequence-www.stanford.edu/group/candida/index.html). This position appears to be paired in a complementary manner for interaction with a Lys in the *mam2* receptor or an Asp in the *C. albicans* receptor at the extracellular end of TMD6.

The rotational orientation of TMD6 and TMD7 in Ste2p is constrained by interaction of a highly conserved residue,

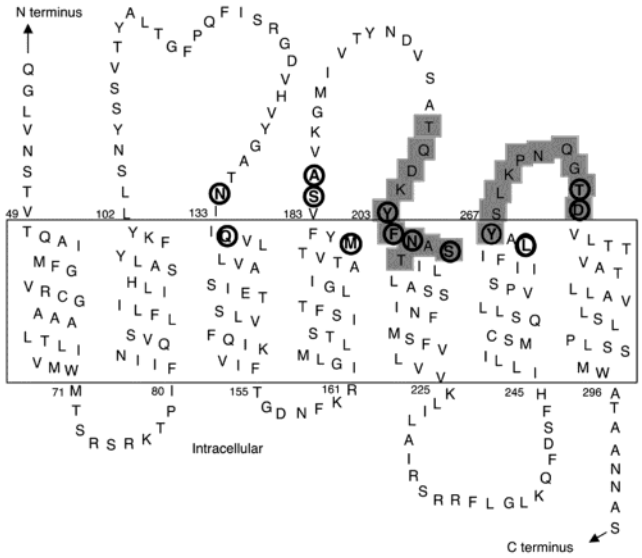

FIGURE 1: Residues near the ends of TMD5 and -6 in the α-factor receptor that were targeted for mutagenesis. Gray boxes denote residues that were substituted with Cys. Circles denote residues affected by dominant-negative mutations (*16*, *17*).

Gln^{253}, with two conserved serine residues on helix 7, Ser^{288} and Ser^{292} (*34*). These serines are part of a motif on helix 7, LPLSSXW, which is highly conserved in the class D GPCRs and may be functionally equivalent to the conserved NPXXY motif in the class A receptors. This orientation of TMD6 places Ser^{254} near Ile^{150} and Ile^{153} on TM3. Substitutions at each of these sites lead to constitutive activity (*7*, *34*).

Once the rotational orientation and the translational position of the transmembrane helices were defined by the genetic, biochemical, and biophysical data described above, the structure was energy minimized using the program XPLOR (*7*). The side chains were placed in standard rotamer conformations. Hydrogen bonding constraints were applied between the backbone amide and carbonyl groups to maintain helical secondary structure. The α-factor receptor has prolines in TMD6 (Pro^{258}) and TMD7 (Pro^{290}). These helices were undistorted in the initial model. Energy minimization resulted in a kink in TMD7 at Pro^{290}, whereas the conformation of TMD6 remained largely undistorted after minimization.

RESULTS

Cysteine Scanning Mutagenesis across Extracellular Ends of TMD5 and -6. The extracellular ends of TMD5 and -6 in the α-factor receptor were targeted for mutagenesis in an effort to better define their role in ligand binding and receptor activation. These studies were prompted by the previous results of genetic screens that identified dominant-negative mutations that affected residues predicted to be near the ends of these TMDs (refs *16* and *17* and summarized in Figure 1), and because TMD5 and -6 are linked by the third intracellular loop, which plays a key role in G protein activation. Therefore, systematic scanning mutagenesis was carried out in which each residue near the predicted extracellular end of TMD5 (residues Thr^{199}−Thr^{208}) and TMD6 (residues Tyr^{266}−Asp^{275}) was mutated to Cys (Figure 1). The 20 Cys substitutions were created in a version of the α-factor receptor gene in which the endogenous Cys codons at positions 59 and 252 were mutated (*8*) to facilitate later analysis of the mutant proteins in biochemical studies.

Table 1: Phenotypes of Cysteine Substitution Mutants

STE2 allele	mating ability[a]	cell division arrest[b]	DN mutation[c]
wild type	+++	+++	
T199C	+++	+++	
Q200C	+++	+++	
D201C	+++	+++	
K202C	+++	+++	
Y203C	+++	+++	Y203H
F204C	sterile	−/DN	F204C, F204S
N205C	+++	partial response	N205D, F205K
A206C	+++	+++	
S207C	+++	+++	S207F
T208C	+++	+++	
Y266C	sterile	−/DN	Y266C, Y266D
S267C	+++	+++	
L268C	+++	+++	
K269C	+++	+++	
P270C	+++	+++	
N271C	+++	+++	
Q272C	+++	+++	
G273C	+++	partial response	
T274C	+++	+++	T274A
D275C	+++	+++	D275V

[a] Ability of strain yLG123 carrying the indicated mutant receptor gene to mate on solid agar medium with MATα strain lys1α. +++, wild-type level of mating; sterile, no detectable mating. [b] Halo assays were used to quantify α-factor-induced cell division arrest. −, no halo; DN, dominant negative in yeast strain JKY25. [c] Dominant-negative mutants identified in previous studies (*16*).

Plasmids containing the Cys mutants were transformed into a yeast strain lacking the chromosomal copy of the receptor gene (*ste2*Δ strain yLG123) for analysis. Western immunoblots showed that all of the mutants produced the expected level of full-length receptor protein (data not shown).

Phenotypes of Cys Mutants. All but two of the receptor mutant strains were able to mate, indicating that most mutants retained some degree of receptor activity (Table 1). In contrast, substitution of Phe[204] (F204C) or Tyr[266] (Y266C) with Cys caused strong defects as these receptor mutants did not stimulate detectable mating. The Cys substitution mutants were next examined in halo assays for the ability to undergo α-factor-induced cell division arrest (Table 1). This is a more stringent test for receptor function because it assays the ability of the mutants to maintain a high level of pheromone response for 2 days. Four of the Cys substitution mutants showed defects in producing a zone of growth inhibition (halo) on an agar plate in response to α-factor (Table 1). As expected from the mating test, the F204C and Y266C mutants did not form a detectable halo, and are thus very insensitive to α-factor. The N205C substitution mutant gave a filled-in halo after 2 days, indicating an inability to maintain a high level of pheromone signaling. The G273C substitution caused cells to form a slightly smaller halo than the wild type, indicating decreased sensitivity to α-factor (Figure 2 and Table 1).

The receptor mutants were tested for dominant phenotypes by introducing the mutant plasmids into a yeast strain (JKY25), which contains a chromosomal copy of wild-type *STE2*. Halo assays showed that the F204C and Y266C mutants dominantly interfered with the ability of the cells to respond to α-factor (Table 1). This was consistent with the previous isolation of F204S and Y266C (or Y266D) mutants in a screen for dominant-negative *STE2* mutants (*16*). The N205C substitution mutant did not cause dominant

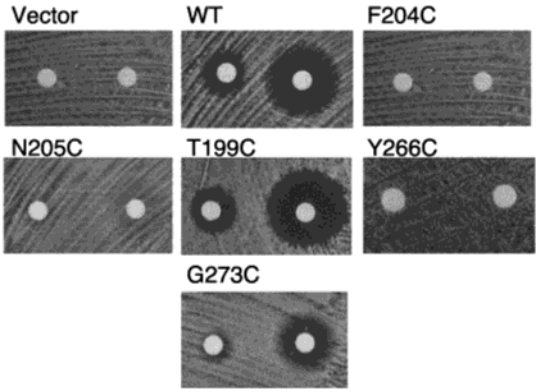

FIGURE 2: Analysis of Cys-substituted mutant receptors. Yeast strain yLG123 carrying the wild-type receptor plasmid or a mutant version containing the indicated Cys substitution was assayed for the ability to undergo cell division arrest in response to α-factor. The zone of growth inhibition (halo) was observed surrounding a filter disk containing α-factor (200 or 1200 ng) that was applied to a lawn of cells on the surface of an agar plate.

effects. This was somewhat surprising since previous studies showed that substitution of Asn[205] with either Asp or Lys caused a dominant-negative phenotype (*16*). The G273C receptor mutants also did not display dominant effects, but this was not unexpected since the effects of this substitution are comparatively mild.

It was interesting that Cys scanning mutagenesis yielded fewer mutants with strong phenotypes than did the random mutagenesis approach used to screen for dominant-negative mutants. For example, substitutions at four other positions near TMD5 or -6 were isolated in the dominant-negative screen (Y203H, S207F, T274A, and D275V), but Cys substitutions at these positions had no detectable effects. However, these results are consistent with previous mutagenesis studies which demonstrated that Cys is generally tolerated well in the α-factor receptor and other proteins (*8*, *23*, *35*). Thus, the strong defects caused by substitution of Phe[204] and Tyr[266] with Cys suggest that they play a special role in receptor function.

Receptor Mutants Respond to an Alternative Agonist. To further define the defects caused by mutating residues 204 and 266, the receptor mutants were tested for their ability to respond to a nonpeptide agonist, novobiocin [*N*-(7-{[3-*O*-(aminocarbonyl)-6-deoxy-5-*C*-methyl-4-*O*-methyl-*β*-L-lyxo-hexopyranosyl]oxy}-4-hydroxy-8-methyl-2-oxo-2*H*-1-benzopyran-3-yl)-4-hydroxy-3-(3-methyl-2-butenyl) benzamide]. Novobiocin was fortuitously identified as an agonist for the α-factor receptor (*36*), but it is more widely known as an inhibitor of bacterial DNA gyrase. Novobiocin is a weak agonist, so the studies were carried out with a strain that is hypersensitive due to deletion of the gene encoding the RGS protein that regulates G protein signaling (*sst2*Δ). Interestingly, both the F204C and F204S receptors responded to novobiocin as well as the wild type in halo assays for cell division arrest (Figure 3A and data not shown). The Y266C receptor mutant strain also responded to novobiocin, but it was ∼5-fold less sensitive to novobiocin than was the wild-type receptor strain. Cells that lack the receptor gene did not respond to novobiocin. In contrast, a control experiment showed that the F204C and Y266C mutants were ∼100-fold less sensitive to α-factor than the wild-type receptor strain (Figure 3B). These results indicate that the

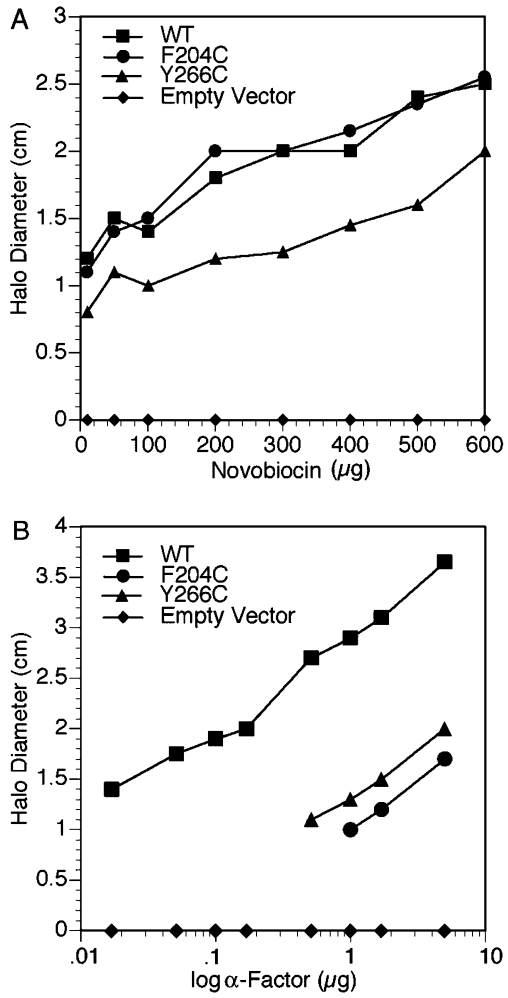

FIGURE 3: Novobiocin activates signaling of F204C and Y266C receptors. Cell division arrest (halo) assays for cells induced with (A) novobiocin or (B) α-factor. Assays were carried out with yeast cells (7416-6-3) carrying a plasmid containing the indicated wild-type or Cys mutant α-factor receptor gene. The indicated amount of ligand was applied to a lawn of cells on solid medium, and then the diameter of the halo was measured after 2 days. The standard deviation was <1.5 mm for each data point.

Ste2p-F204C and -Y266C receptors are specifically defective in responding to α-factor, and are not grossly misfolded. Thus, taken together with the observation that the F204S mutant is defective in α-factor binding (*16*), these results suggest that Phe^{204} may play a direct role in binding α-factor. In contrast, the Y266C mutant displays an only ~2.5-fold lower binding affinity for α-factor than the wild-type receptor (*16*), consistent with the Tyr^{266} residue being primarily important for promoting the activated receptor state.

Accessibility of Substituted Cys Residues. Hydropathy analysis predicts that Phe^{204} and Tyr^{266} reside near the ends of the TMDs (*37*). However, the extracellular boundaries of the TMDs are not defined, so it is unclear whether these residues are accessible on the surface or buried in the membrane. To gain further insight into how Phe^{204} and Tyr^{266} contribute to receptor signaling, we investigated the boundaries of the TMDs by testing the accessibility of Cys-substituted residues in the mutants to a thiol-reactive probe that is membrane-impermeable (MTSEA-biotin). The α-factor receptor is well-suited for this approach because, in contrast to many other GPCRs, it lacks essential Cys residues. In particular, it does not contain the pair of conserved Cys residues that form a disulfide bond between the second extracellular loop and the extracellular end of TMD3 in many GPCRs. The two endogenous Cys residues at positions 59 and 252 are not essential and were therefore replaced to create a version of the α-factor receptor lacking Cys residues that is considered to be the wild type for these studies (*8*).

The accessibility assays were carried out by treating membrane fractions with MTSEA-biotin, solubilizing the proteins in detergent buffer, and then collecting the biotin-labeled receptors on streptavidin beads (see Materials and Methods). The degree of receptor biotinylation was determined by comparing samples of the total extract, the streptavidin bead supernatant, and the eluted proteins on Western immunoblots. Control experiments showed that the wild-type receptors lacking Cys residues were present only at low levels (1.6%) in the fraction bound to strepavidin beads, indicating that they did not react significantly with MTSEA-biotin (Figure 4A). In contrast, the T199C receptors, which contain a Cys at a position that is thought to be in the second extracellular loop, reacted significantly with MTSEA-biotin (26%). This level of biotinylation may be an underestimate since stringent washing conditions were used to prevent nonspecific sticking to the streptavidin beads. Other control experiments showed that the binding to the streptavidin beads was only detectable after MTSEA-biotin treatment (Figure 4B). A Western blot probed with horseradish peroxidase-conjugated streptavidin confirmed that all of the membrane samples reacted with MTSEA-biotin, and that the biotinylated proteins were depleted from the supernatant fractions, indicating they bound efficiently to the streptavidin beads (Figure 4C). We also showed that a mutant receptor (Y266C) that does not react detectably with MTSEA-biotin in this assay format could do so if it was first extracted from the membrane with detergent buffer prior to the analysis (Figure 4D).

Twenty-seven Cys mutants were analyzed, including those constructed in this study and some additional mutants that were made in a previous study (*8*). Quantitative analysis showed that 15 mutants were biotinylated to essentially the same level as T199C receptors, indicating that they are accessible to MTSEA-biotin (Figure 5 and Table 2). Interestingly, all of the accessible residues corresponded to those that were predicted to be furthest out in the extracellular domain. In contrast, the five mutants that were not efficiently biotinylated all contained Cys residues that were predicted to be most deeply buried in the membrane. The seven remaining mutants showed intermediate levels of biotinylation, and all of these mapped to the interface region. Addition of α-factor did not cause an obvious change in the accessibility to MTSEA-biotin (data not shown).

In TMD6, the drop in the level of biotinylation occurred between K269C and L268C. There was a rapid drop in accessibility over two residues that marked the interface region. In contrast, the drop in the level of biotinylation of TMD5 occurred over six residues between S206C and A212C. Perhaps this difference reflects the greater flexibility of TMD5 residues (see the Discussion). These data are interesting in that they predict that Phe^{204} is on the surface-accessible side of the boundary, consistent with it playing a direct role in ligand binding. On the other hand, Tyr^{266} is apparently not surface-accessible, suggesting that it carries

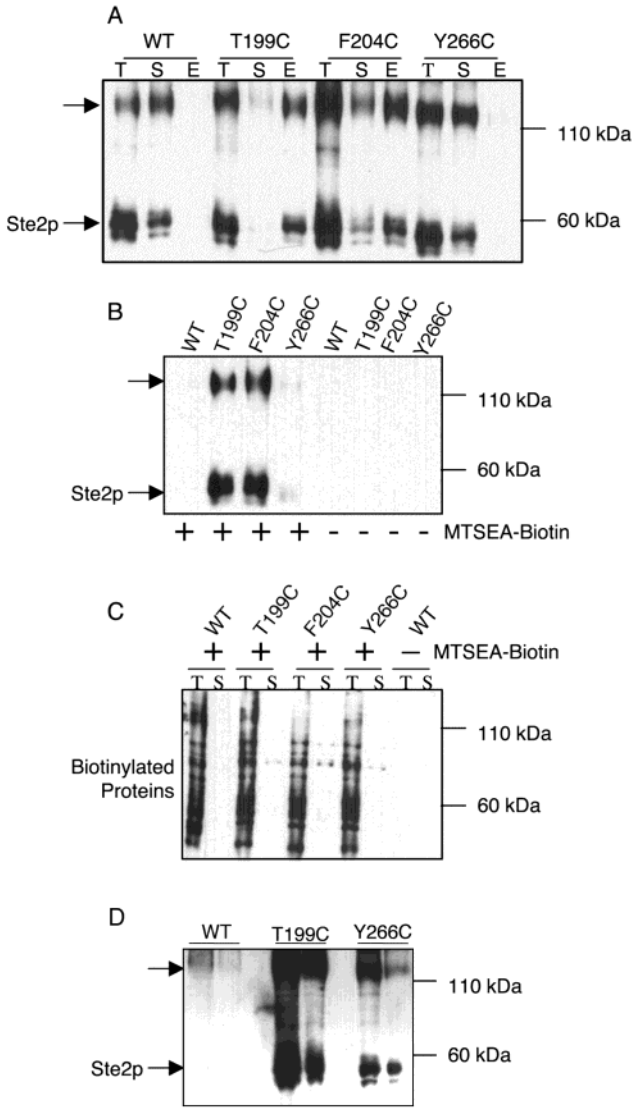

FIGURE 4: Reaction of receptors with MTSEA-biotin. (A and B) Western blot analysis of the indicated wild-type or mutant α-factor receptor proteins detected with anti-HA antibody. (A) Cell membranes were treated with MTSEA-biotin, and then equal fractions of the total membrane extract (T), streptavidin bead supernatant (S), and eluate (E) fractions were analyzed. Arrows point to monomer and apparent dimer forms of the receptor protein (Ste2p). (B) Cell membranes were incubated with or without MTSEA-biotin, and then the proteins that eluted from the streptavidin beads were analyzed on the blot. (C) Total biotinylated proteins were detected on a Western blot probed with streptavidin conjugated to horseradish peroxidase. The blot contains the total membrane extract and the supernatant fraction from the streptavidin beads. (D) Reaction of detergent-extracted receptors with MTSEA-biotin. Membrane fractions from 10^7 cells were extracted with detergent buffer and reacted with MTSEA-biotin, and then the biotinylated Ste2p was collected on streptavidin beads. Fractions corresponding to 60 and 20% of the material eluted from the streptavidin beads were analyzed for each of the indicated receptor types on a Western blot probed with anti-HA antibodies.

out a step in receptor activation that occurs within the membrane bilayer.

DISCUSSION

The study of GPCR activation is complicated by the ability of ligands to form multiple contacts with the various TMDs and extracellular regions (*12*). This is particularly true for larger ligands such as peptides or polypeptides. Therefore, it was interesting that a cluster of dominant-negative α-factor receptor mutations implicated the extracellular ends of TMDs in signaling (*16*−*18*). The dominant mutants are defective in responding to α-factor, but retained partial function in that they were apparently able to sequester G proteins into preactivation complexes (*16*, *19*). Consistent with this set of mutants identifying a domain critical for receptor activation, the strongest mutants affected Phe^{204} and Tyr^{266} near the ends of TMD5 and -6. These TMDs are linked by the third intracellular loop, which plays a key role in G protein activation (*21*, *22*).

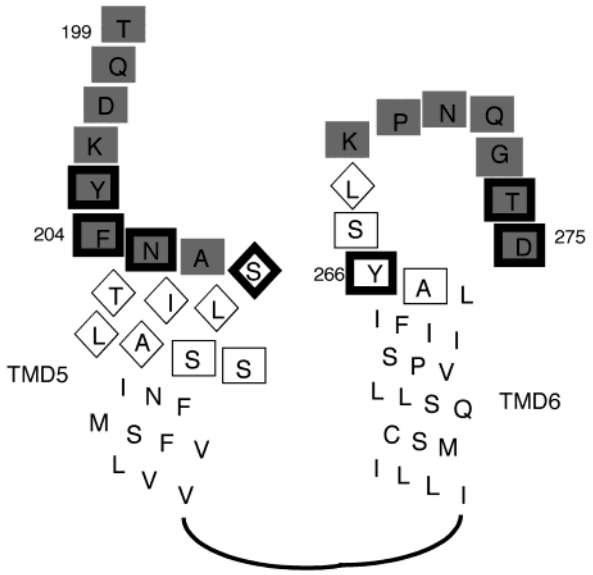

FIGURE 5: Accessibility of residues near the ends of TMD5 and -6. Gray boxes denote accessible residues that reacted most strongly with MTSEA-biotin. White boxes denote residues that reacted poorly. Diamond boxes denote intermediate reactivity. Boxes and the diamond with thick outlines identify residues affected by dominant-negative mutations.

Table 2: MTSEA-Biotin Reaction with Cysteine Substitution Mutants

TMD5 *STE2* allele	relative biotinylation (%)[a]	TMD6 *STE2* allele	relative biotinylation (%)[a]
wild type	8.3 ± 11	D275C	88.3 ± 36
T199C	100	T274C	77 ± 16
Q200C	100.2 ± 36	G273C	74.5 ± 12
D201C	100.8 ± 43	Q272C	92.5 ± 19
K202C	93 ± 13	N271C	81.2 ± 26
Y203C	151.5 ± 18	P270C	131.8 ± 84
F204C	90 ± 29	K269C	91.8 ± 13
N205C	74.8 ± 38	L268C	36.3 ± 6
A206C	69.8 ± 33	S267C	11.8 ± 15
S207C	37.2 ± 6	Y266C	15 ± 10
T208C	49 ± 18	A265C	15 ± 7
I209C	40 ± 35		
L210C	36.1 ± 14		
L211C	34.3 ± 17		
A212C	28.7 ± 12		
S213C	17 ± 2		
S214C	16 ± 12		

[a] Indicated Cys-substituted receptors were reacted with MTSEA-biotin, and then the degree of biotinylation was quantified as described in Materials and Methods. The degree of receptor biotinylation is reported relative to that of T199C receptors which were normalized to 100%.

Cys Scanning Mutagenesis Implicates Phe[204] and Tyr[266]. Systematic mutagenesis of each residue near the ends of TMD5 and -6 of the α-factor receptor showed that substitution of Phe[204] or Tyr[266] with Cys caused a severe defect in signaling (Figure 2). Phe[204] and Tyr[266] are specific for α-factor-induced signaling because they retained the ability to respond to a different agonist, novobiocin (Figure 3). Furthermore, Cys substitution of the other 25 residues examined in this region did not strongly disrupt receptor function. This included six positions that were shown previously to cause dominant-negative effects when substituted with other residues (i.e., Ste2p-Y203H, -N205K, -S207F, -L264P, -T274A, and -D275V). This latter subset of residues may not play a specific role in signaling, but may be close to a critical domain such that certain substitutions perturb receptor function. Consistent with this, many of the substitutions dramatically changed the character of the side chain in this subset of dominant-negative mutants. In contrast, Phe[204] and Tyr[266] appear to be specifically involved in α-factor-dependent signaling.

TMD Boundaries. Hydropathy analysis predicts that Phe[204] and Tyr[266] are near the ends of the TMDs. However, computer models vary considerably in predicting the ends of the TMDs. More precise information has been obtained by spin-labeling methods to determine the solvent accessibility of selected residues in rhodopsin (*38*), for which there are efficient approaches for this analysis, but the TMD boundaries are not defined for other GPCRs. Therefore, we modified the substituted cysteine accessibility method (SCAM) to determine which residues in the α-factor receptor are accessible to the membrane-impermeable probe MTSEA-biotin (Figure 4). SCAM employs thiol-reactive methane thiosulfonate reagents developed by Karlin's group (*39*) that have been used widely to define the presence of accessible loops or to probe the residues that line a pore in polytopic membrane proteins (*23*, *40*, *41*). Thus, the methods employed in this study should have application in the analysis of the TMDs of other membrane proteins.

In TMD6, the reactivity of Cys-substituted α-factor receptors with MTSEA-biotin dropped off sharply over two residues (267 and 268). This trend of residues decreasing in accessibility to MTSEA-biotin suggests that this likely corresponds to the start of the core region of TMD6 that is buried in the membrane (Figure 5). For TMD5, the drop in reactivity occurred more gradually over six residues (from 207 to 212). This may indicate that TMD5 is more flexible, a possibility that is consistent with genetic evidence that TMD6 is restrained by interaction with TMD3 and -7 in the α-factor receptor (*7*, *34*). Alternatively, this effect could be due to other local differences in conformation of these TMDs that permits greater access for MTSEA-biotin. However, there were clear transition points in both TMD5 and TMD6 that provide the first experimental evidence for the boundaries of the TMDs in the α-factor receptor. These results are in general agreement with the predicted boundaries based on previous genetic and chemical cross-linking data (*8*). The MTSEA-biotin accessibility data therefore provide important new insights into the role of specific residues. In particular, the accessibility of Cys at position 204 provides support for Phe[204] playing a direct role in ligand binding, as was suggested by the defect in binding α-factor that is caused by mutating this residue (*16*). In contrast, the apparent

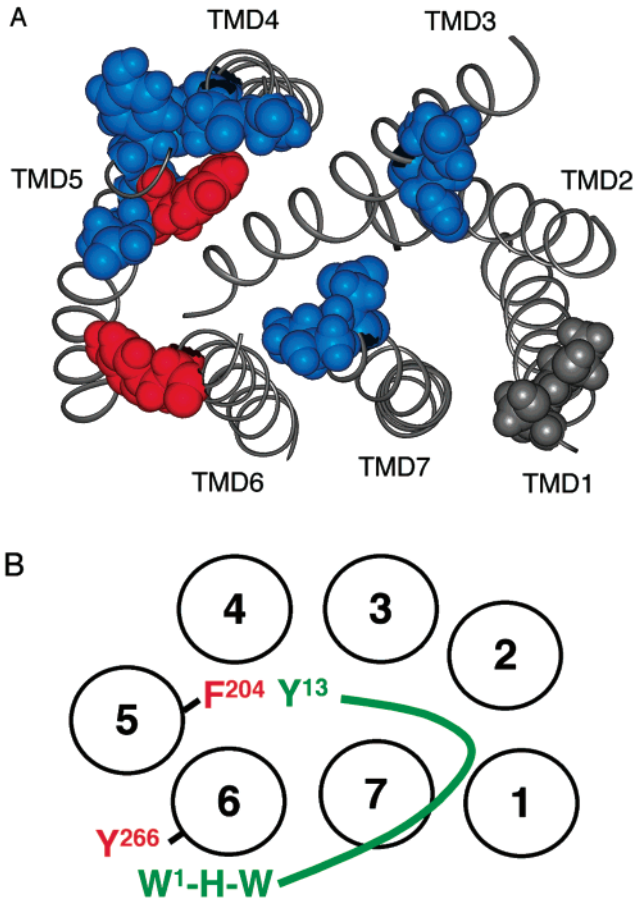

FIGURE 6: α-Factor receptor models. (A) Three-dimensional molecular model of the α-factor receptor. Extracellular view of the α-factor receptor transmembrane region (gray ribbons) showing residues affected by dominant-negative mutations (*16*−*18*). Phe[204] and Tyr[266] are shown with red van der Waals surfaces. The other residues affected by dominant-negative mutations are shown with blue van der Waals surfaces. Ser[47] and Thr[48] at the end of TMD1 have been implicated in ligand binding (*42*) and are shown with gray van der Waals surfaces. (B) Schematic representation of a model for the binding of α-factor to its receptor.

inaccessibility of Tyr[266] correlates with this residue not playing a major role in ligand binding affinity and instead playing a subsequent role in receptor activation.

Model for Receptor Activation. To better understand how Phe[204] and Tyr[266] function in receptor activation, a three-dimensional molecular model of the TMDs of the α-factor receptor was developed (Figure 6A). This model was created by mapping the residues of the α-factor receptor onto a α-carbon template of the TMDs of the photoreceptor rhodopsin (see Materials and Methods). The amino acids affected by the dominant-negative mutations cluster at the extracellular ends of TMD3−7, suggesting that this region plays a key role in agonist activation. They lie roughly in the same plane and, with the notable exception of Tyr[266], are oriented in toward the helix interfaces or the interior of the helix bundle. The residues affected by dominant-negative mutants on the ends of TMD4 and -5 are packed together, and the residues on the ends of TMD3 and TMD7 have the potential of interacting. Tyr[266] on TMD6 is clearly oriented toward the surrounding lipids, while Phe[204] is located within the helix bundle between TMD4 and -5. Ser[47] and Thr[48] (gray van der Waals surfaces), which are predicted to be near the extracellular end of TMD1 and facing the interior of the helix

bundle, have been implicated in ligand binding (*42*). Ser^{47} and Thr^{48} may interact directly with the ligand or with the amino acids affected by dominant-negative mutants at the end of TMD7 (depending on the magnitude of the kink caused by Pro^{290}). Thus, a pocket formed by the ends of the TMDs seems likely to play a key role in α-factor binding and receptor activation. The predicted length of this pocket in the interior of the helix bundle from TMD1 to TMD5 is ~15 Å, and is ~35 Å when measured from the outer sides of these TMDs that face the lipid bilayer (Figure 6). As an extended peptide, α-factor (~50 Å) would be more than long enough to fit into the pocket and to interact with Tyr^{266} which is oriented away from the helical bundle and is inaccessible to MTSEA-biotin.

To interact with the cluster of amino acids identified by the dominant-negative mutants, α-factor may be bent such that the N- and C-termini are in proximity. A *β*-bend has previously been proposed at the Pro^{8}-Gly^{9} sequence (*43*). Interestingly, similar phenotypes caused by mutating certain aromatic residues in either the ligand or the receptor suggest the possibility that the implicated residues directly interact (*4*, *16*, *44*). For example, mutation of either Phe^{204} in the receptor or Tyr^{13} in the α-factor ligand causes a strong defect in binding affinity. In contrast, mutation of either Tyr^{266} in the receptor or the Trp residues at positions 1 and 3 in the α-factor ligand does not strongly affect binding, but diminishes the degree of signaling. In fact, an α-factor that lacks these Trp residues (des-Trp^{1}, Ala^{3}) acts as an antagonist (*45*, *46*). Thus, Phe^{204} is functionally similar to the C-terminus of α-factor, and Tyr^{266} is functionally similar to the N-terminal residues. Although Trp^{1} and Tyr^{13} are at opposite ends of the α-factor ligand, and Phe^{204} and Tyr^{266} are on adjacent TMDs, a bend in α-factor should bring the corresponding residues into proximity (Figure 6B). Consistent with this model, the amino terminus of α-factor could be chemically cross-linked to a region of the receptor that contains TMD6 and TMD7 (*47*).

Interaction between aromatic residues in the α-factor ligand and its receptor could be stabilized by ring stacking effects or by hydrogen bonding. Since Phe^{204} on the receptor appears to be accessible, it could stably interact with Tyr^{13} of the α-factor ligand. In contrast, Tyr^{266} was not accessible to MTSEA-biotin either in the presence or in the absence of α-factor. If the Trp residues in the N-terminus of α-factor do in fact interact with Tyr^{266}, they would apparently have to insert into the membrane bilayer. This assumes that the rotational orientation of TMD6 (see Materials and Methods) is correct and Tyr^{266} is oriented away from the helix bundle. Association of the N-terminal Trp-His-Trp sequence with phospholipid membranes is indirectly supported by a wide range of model compound studies on peptides with basic and aromatic residues (*29*, *48*, *49*). Aromatic residues preferentially partition into the headgroup region of phospholipid bilayers (*29*, *48*), and basic residues interact electrostatically with the negatively charged phospholipid headgroup acids (*49*). Direct support for the possibility that the N-terminus of α-factor can insert into membranes comes from NMR studies (*50*). Altogether, these results highlight the special role that aromatic residues play in promoting the interaction between α-factor and the ends of the TMDs in the receptor.

Implication for Other GPCRs. The discovery that the extracellular ends of TMDs function as a microdomain in the α-factor receptor has important implications for other GPCRs. Previous mutational or affinity labeling studies of other receptors have frequently identified residues near the extracellular ends of TMDs that are involved in binding of peptide ligands such as C5a, angiotensin II, and cholecystokinin (*12*, *51*−*54*). Furthermore, creation of a metal binding site at the extracellular ends of TMD3 and -7 of either the β_2-adrenergic or tachykinin receptors caused metal-dependent receptor activation (*55*, *56*), whereas creation of a metal-binding site at the extracellular ends of TMD5 and -6 of the tachykinin receptor blocked receptor signaling (*57*). In addition, aromatic residues near the extracellular ends of TMDs have also been suggested to participate in the binding of small ligands (*12*, *58*). One of the most striking correlations is the similarity in functional microdomains in TMD6 between rhodopsin and the α-factor receptor. Tyr^{266} in the α-factor receptor correlates functionally with Tyr^{268} in TMD6 of rhodopsin. Both Tyr^{266} and Tyr^{268} appear to couple ligand binding to a conformational change in the receptor. Mutational analysis indicates that Tyr^{268} is in van der Waals contact with the retinal chromophore and is needed for efficient transducin activation (*59*, *60*); Tyr^{266} is thought to interact with the peptide ligand of Ste2p. These results indicate that aromatic residues at the extracellular ends of the TMDs are critical for function in a wide range of GPCRs.

REFERENCES

1. Elion, E. A. (2000) *Curr. Opin. Microbiol. 3*, 573−581.
2. Dohlman, H. G., and Thorner, J. W. (2001) *Annu. Rev. Biochem. 70*, 703−754.
3. Ballesteros, J. A., Shi, L., and Javitch, J. A. (2001) *Mol. Pharmacol. 60*, 1−19.
4. Abel, M. G., Zhang, Y. L., Lu, H. F., Naider, F., and Becker, J. M. (1998) *J. Pept. Res. 52*, 95−106.
5. Jenness, D. D., Burkholder, A. C., and Hartwell, L. H. (1983) *Cell 35*, 521−529.
6. Whiteway, M., Hougan, L., Dignard, D., Thomas, D. Y., Bell, L., Saari, G. C., Grant, F. J., O'Hara, P., and MacKay, V. L. (1989) *Cell 56*, 467−477.
7. Parrish, W., Eilers, M., Ying, W., and Konopka, J. B. (2002) *Genetics 160*, 429−443.
8. Dube, P., DeConstanzo, A., and Konopka, J. B. (2000) *J. Biol. Chem. 275*, 26492−26499.
9. Crowe, M. L., Perry, B. N., and Connerton, I. F. (2000) *J. Recept. Signal Transduction Res. 20*, 61−73.
10. Pausch, M. H. (1997) *Trends Biotechnol. 15*, 487−494.
11. Broach, J. R., and Thorner, J. (1996) *Nature 384*, 14−16.
12. Ji, T. H., Grossmann, M., and Ji, I. (1998) *J. Biol. Chem. 273*, 17299−17302.
13. Konopka, J. B., Jenness, D. D., and Hartwell, L. H. (1988) *Cell 54*, 609−620.
14. Reneke, J. E., Blumer, K. J., Courchesne, W. E., and Thorner, J. (1988) *Cell 55*, 221−234.
15. Sen, M., and Marsh, L. (1994) *J. Biol. Chem. 269*, 968−973.
16. Dosil, M., Giot, L., Davis, C., and Konopka, J. B. (1998) *Mol. Cell. Biol. 18*, 5981−5991.
17. Yesilaltay, A., and Jenness, D. D. (2000) *Mol. Biol. Cell 11*, 2873−2884.
18. Leavitt, L. M., Macaluso, C. R., Kim, K. S., Martin, N. P., and Dumont, M. E. (1999) *Mol. Gen. Genet. 261*, 917−932.
19. Dosil, M., Schandel, K., Gupta, E., Jenness, D. D., and Konopka, J. B. (2000) *Mol. Cell. Biol. 20*, 5321−5329.
20. Martin, N. P., Celic, A., and Dumont, M. E. (2002) *J. Mol. Biol. 317*, 765−788.
21. Schandel, K. A., and Jenness, D. D. (1994) *Mol. Cell. Biol. 14*, 7245−7255.
22. Stefan, C. J., and Blumer, K. J. (1994) *Mol. Cell. Biol. 14*, 3339−3349.

23. Karlin, A., and Akabas, M. H. (1998) *Methods Enzymol. 293*, 123−145.
24. Sherman, F. (1991) *Methods Enzymol. 194*, 3−21.
25. Schiestl, R. H., and Gietz, R. D. (1989) *Curr. Genet. 16*, 339−346.
26. Palczewski, K., Kumasaka, T., Hori, T., Behnke, C. A., Motoshima, H., Fox, B. A., Le Trong, I., Teller, D. C., Okada, T., Stenkamp, R. E., Yamamoto, M., and Miyano, M. (2000) *Science 289*, 739−745.
27. Zhang, D., and Weinstein, H. (1993) *J. Med. Chem. 36*, 934−938.
28. Adamian, L., and Liang, J. (2001) *J. Mol. Biol. 311*, 891−907.
29. Wimley, W. C., and White, S. H. (1996) *Nat. Struct. Biol. 10*, 842−848.
30. Visiers, I., Ballesteros, J. A., and Weinstein, H. (2002) *Methods Enzymol. 343*, 329−371.
31. Eilers, M., Patel, A. B., Liu, W., and Smith, S. O. (2002) *Biophys. J. 82*, 2720−2736.
32. Sommers, C. M., Martin, N. P., Akal-Strader, A., Becker, J. M., Naider, F., and Dumont, M. E. (2000) *Biochemistry 39*, 6898−6909.
33. Kitamura, K., and Shimoda, C. (1991) *EMBO J. 10*, 3743−3751.
34. Dube, P., and Konopka, J. B. (1998) *Mol. Cell. Biol. 18*, 7205−7215.
35. Frillingos, S., Sahin-Toth, M., Wu, J., and Kaback, H. R. (1998) *FASEB J. 12*, 1281−1299.
36. Pocklington, M. J., and Orr, E. (1994) *Biochim. Biophys. Acta 1224*, 401−412.
37. Burkholder, A. C., and Hartwell, L. H. (1985) *Nucleic Acids Res. 13*, 8463−8475.
38. Altenbach, C., Klein-Seetharaman, J., Hwa, J., Khorana, H. G., and Hubbell, W. L. (1999) *Biochemistry 38*, 7945−7949.
39. Akabas, M. H., Stauffer, D. A., Xu, M., and Karlin, A. (1992) *Science 258*, 307−310.
40. Javitch, J. A., Li, X., Kaback, J., and Karlin, A. (1994) *Proc. Natl. Acad. Sci. U.S.A. 91*, 10355−10359.
41. Chen, J. G., Liu-Chen, S., and Rudnick, G. (1998) *J. Biol. Chem. 273*, 12675−12681.
42. Lee, B. K., Khare, S., Naider, F., and Becker, J. M. (2001) *J. Biol. Chem. 276*, 37950−37961.
43. Zhang, Y. L., Marepalli, H. R., Lu, H. F., Becker, J. M., and Naider, F. (1998) *Biochemistry 37*, 12465−12476.
44. Manfredi, J. P., Klein, C., Herrero, J. J., Byrd, D. R., Trueheart, J., Wiesler, W. T., Fowlkes, D. M., and Broach, J. R. (1996) *Mol. Cell. Biol. 16*, 4700−4709.
45. Raths, S. K., Naider, F., and Becker, J. M. (1988) *J. Biol. Chem. 263*, 17333−17341.
46. Shenbagamurthi, P., Baffi, R., Khan, S. A., Lipke, P., Pousman, C., Becker, J. M., and Naider, F. (1983) *Biochemistry 22*, 1298−1304.
47. Henry, L. K., Khare, S., Son, C., Babu, V. V., Naider, F., and Becker, J. M. (2002) *Biochemistry 41*, 6128−6139.
48. Yau, W. M., Wimley, W. C., Gawrisch, K., and White, S. H. (1998) *Biochemistry 37*, 14713−14718.
49. Murray, D., Arbuzova, A., Honig, B., and McLaughlin, S. (2002) *Curr. Top. Membr. 52*, 271−302.
50. Wakamatsu, K., Okada, A., Miyazawa, T., Masui, Y., Sakakibara, S., and Higashijima, T. (1987) *Eur. J. Biochem. 163*, 331−338.
51. Baranski, T. J., Herzmark, P., Lichtarge, O., Gerber, B. O., Trueheart, J., Meng, E. C., Iiri, T., Sheikh, S. P., and Bourne, H. R. (1999) *J. Biol. Chem. 274*, 15757−15765.
52. Ding, X. Q., and Miller, L. J. (2001) *Peptides 22*, 1223−1228.
53. Hunyady, L., Balla, T., and Catt, K. J. (1996) *Trends Pharmacol. Sci. 17*, 135−140.
54. Meng, E. C., and Bourne, H. R. (2001) *Trends Pharmacol. Sci. 22*, 587−593.
55. Holst, B., Elling, C. E., and Schwartz, T. W. (2000) *Mol. Pharmacol. 58*, 263−270.
56. Elling, C. E., Thirstrup, K., Holst, B., and Schwartz, T. W. (1999) *Proc. Natl. Acad. Sci. U.S.A. 96*, 12322−12327.
57. Elling, C. E., Nielsen, S. M., and Schwartz, T. W. (1995) *Nature 374*, 74−77.
58. Wess, J., Blin, N., Mutschler, E., and Bluml, K. (1995) *Life Sci. 56*, 915−922.
59. Nakayama, T. A., and Khorana, H. G. (1991) *J. Biol. Chem. 266*, 4269−4275.
60. Ridge, K. D., Bhattacharya, S., Nakayama, T. A., and Khorana, H. G. (1992) *J. Biol. Chem. 267*, 6770−6775.

BI026766O